5-1-2010

Observation Of A Nonaxisymmetric Magnetohydrodynamic Self-Organized State

C. D. Cothran

Michael R. Brown
Swarthmore College, doc@swarthmore.edu

T. Gray

M. J. Schaffer

G. Marklin

See next page for additional authors

Observation of a nonaxisymmetric magnetohydrodynamic self-organized statea)

C. D. Cothran, M. R. Brown, T. Gray, M. J. Schaffer, G. Marklin, and V. S. Lukin

Citation: Physics of Plasmas (1994-present) **17**, 055705 (2010); doi: 10.1063/1.3327214
View online: http://dx.doi.org/10.1063/1.3327214
View Table of Contents: http://scitation.aip.org/content/aip/journal/pop/17/5?ver=pdfcov
Published by the AIP Publishing

Observation of a nonaxisymmetric magnetohydrodynamic self-organized state[a)]

C. D. Cothran,[1,b)] M. R. Brown,[1] T. Gray,[1] M. J. Schaffer,[2] G. Marklin,[3] and V. S. Lukin[4]
[1]*Swarthmore College, Swarthmore, Pennsylvania 19081, USA*
[2]*General Atomics, San Diego, California 92186, USA*
[3]*University of Washington, Seattle, Washington 98195, USA*
[4]*Space Sciences Division, U. S. Naval Research Laboratory, Washington, DC 20375, USA*

(Received 20 November 2009; accepted 29 January 2010; published online 30 March 2010)

A nonaxisymmetric stable magnetohydrodynamic (MHD) equilibrium within a prolate cylindrical conducting boundary has been produced experimentally at Swarthmore Spheromak Experiment (SSX) [M. R. Brown *et al.*, Phys. Plasmas **6**, 1717 (1999)]. It has $m=1$ toroidal symmetry, helical distortion, and flat λ profile. Each of these observed characteristics are in agreement with the magnetically relaxed minimum magnetic energy Taylor state. The Taylor state is computed using the methods described by A. Bondeson *et al.* [Phys. Fluids **24**, 1682 (1981)] and by J. M. Finn *et al.* [Phys. Fluids **24**, 1336 (1981)] and is compared in detail to the measured internal magnetic structure. The lifetime of this nonaxisymmetric compact torus (CT) is comparable to or greater than that of the axisymmetric CTs produced at SSX; thus suggesting confinement is not degraded by its nonaxisymmetry. For both one- and two-spheromak initial state plasmas, this same equilibrium consistently emerges as the final state. © *2010 American Institute of Physics*.
[doi:10.1063/1.3327214]

I. INTRODUCTION

Spheromak[1–5] and reversed-field pinch (RFP) (Ref. 6) plasmas (as well as other more exotic configurations[7]) are well described by Taylor relaxation theory.[8,9] Even for initial conditions very far from equilibrium, these plasmas will settle to stable magnetic configurations dependent only on the shape of their conducting boundary and the total magnetic helicity initially present in the plasma (and, in the case of the RFP, the toroidal flux). Taylor's proposal that the dynamics of these plasmas conserve the total helicity while seeking a state of minimum magnetic energy leads to the condition that such "relaxed" states satisfy

$$\nabla \times \vec{B} = \lambda \vec{B}, \tag{1}$$

where λ is a constant. Taylor states are therefore force-free ($\vec{J} \times \vec{B} = 0$) but with a spatially invariant ratio of J/B. This important characteristic indicates the relaxed nature of the plasma and its insensitivity to the details of the initial conditions that would otherwise be preserved if the plasma obeyed ideal magnetohydrodynamics (MHD). The inclusion of even a small amount of resistivity is essential. Taylor envisioned a turbulent relaxation process where reconnection occurred on small scales to render meaningless the infinite number of ideally conserved helicities of individual flux tubes, so that the only possible ideal invariant preserved for a real (resistive) plasma would be the total helicity.

Magnetic relaxation is considered to be an example of self-organization: the tendency for large scale structure to appear in a variety of physical systems. Hasegawa[10] reviewed how systems as diverse as optical solitons, zonal flows in rotating planetary atmospheres, two-dimensional fluid,[11] as well as MHD turbulence (as Taylor presumed for relaxation dynamics) have been shown to be self-organizing as a consequence of their general properties as dissipative continuous systems with more than one ideal invariant.

This paper provides further description of a nonaxisymmetric magnetically relaxed (self-organized) plasma[12] produced within an elongated cylindrical conducting boundary. The internal magnetic structure of this compact torus (CT) plasma is measured in detail and found to contain a helical distortion and pure azimuthal (toroidal) $m=1$ symmetry. A general method[13,14] to calculate the Taylor state within a cylindrical boundary is reviewed and the states for large aspect ratio (length L to radius R) are analyzed; for the $L/R=3$ aspect ratio of the experiment, the Taylor state structure agrees well with the measured structure. Furthermore, the spatial profile of lambda is measured to be roughly flat and consistent with the constant value computed for the Taylor state. The experiment can be started with either one or two-spheromak plasmas, yet the same self-organized state appears following a period of strong MHD activity.

II. EXPERIMENT

A sketch containing the essential elements of the Swarthmore Spheromak Experiment (SSX) (Ref. 15) is shown in Fig. 1. Pulsed-power driven coaxial magnetized plasma guns produce hydrogen spheromaks on either end of a conducting (copper) cylindrical boundary of length $L=63$ cm and radius $R=20$ cm. The cylindrical boundary is split at the midplane for diagnostic access, but each half is electrically connected via the outer electrodes of the plasma guns and the vacuum chamber (not shown in Fig. 1). The

[a)]Paper XI3 6, Bull. Am. Phys. Soc. **54**, 345 (2009).
[b)]Invited speaker. Present address: Global Strategies Group (North America). Electronic mail: cothran.c@gmail.com.

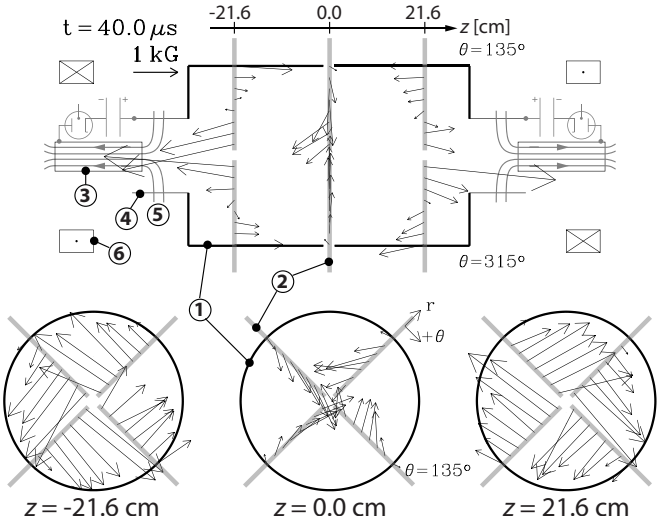

FIG. 1. Sketch of the SSX device. Numbers indicate the following: (1) the $L/R=3.0$ cylindrical conducting boundary with $R=20$ cm; (2) one of 12 linear magnetic probe arrays inserted radially into the device; and for one of the two plasma guns on each end of the device, the (3) inner and (4) outer coaxial electrodes linked by (5) magnetic flux from (6) an external coil (the ignitron switched capacitor banks are also indicated schematically). Each magnetic probe array makes eight $\vec{B}$ measurements with radial spacing of 2.5 cm. The full set of twelve probes determines three right circular cross sections of the cylindrical plasma volume at $z=-21.6$ cm, $z=0.0$ cm, and $z=+21.6$ cm, each with four probes equally spaced azimuthally (i.e., at $\theta=45°$, 135°, 225°, and 315°), in addition to two rz planes of data. Only one rz plane of $\vec{B}$ data is shown in this figure since at this early time ($t=40$ μs, where initiation of the discharge defines $t=0$) the two right-handed spheromaks have not interacted much and are largely axisymmetric.

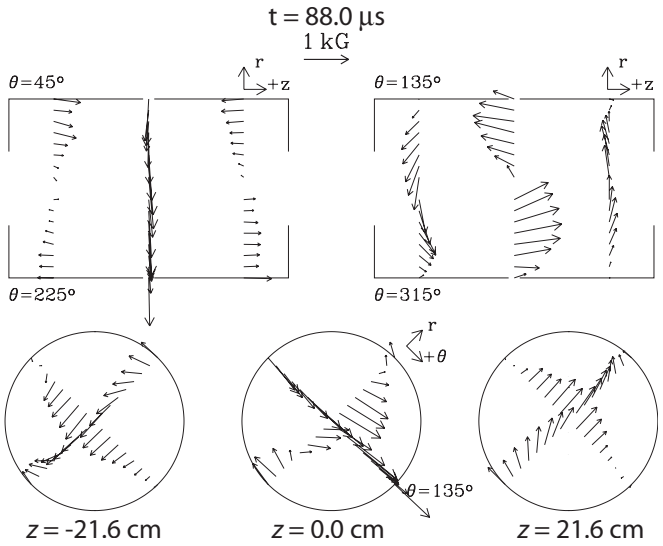

FIG. 2. The measured magnetic structure of the relaxed state at $t=88$ μs, following the completion of the cohelicity merging process. The mostly axisymmetric initial state containing two spheromaks is shown in Fig. 1. Both rz planes of data are shown since this state is inherently nonaxisymmetric.

plasma guns are independent so that one or both can be operated for a given experiment. The polarity of the magnetic coil on each gun controls the sign of the helicity of the spheromak produced. For the two-spheromak experiments described here, the guns produced spheromaks of roughly the same magnitude and sign of helicity; this is referred to as a cohelicity merging experiment.[16]

Twelve linear magnetic probes are inserted radially for internal magnetic structure measurements. Each linear probe makes eight $\vec{B}$ measurements spaced 2.5 cm radially. The time resolution of these measurements is 0.8 μs, sufficient to track the MHD timescale evolution of the plasma. Sets of four are located at the midplane ($z=0$) and at $z=\pm 21.6$ cm with each set equally spaced azimuthally. Subsequent analysis will rely on the azimuthal Fourier decomposition of the data from each set of four probes. The $m=0$ (axisymmetric) and $m=1$ modes can be fully resolved and the $m=2$ mode is partially resolved.

The diagnostics used for these experiments including the magnetic probes are the same as those described in Ref. 17 with the addition of a fast high spectral resolution ion Doppler spectroscopy (IDS) instrument.[18] Plasma conditions are monitored by quadrature interferometry for electron density n_e and with the IDS instrument to determine the carbon (impurity) ion temperature T_i. Note that the IDS measurements were made with the magnetic probes removed from the plasma. Magnetic measurements have an uncertainty of about 20 G and systematic error from phase drift in the n_e measurement is estimated at less than $1\times10^{14}/\text{cm}^3$. Gaussian lineshape fitting determines T_i and its uncertainty; the minimum resolvable T_i (the "instrument temperature" associated with the spectral resolution) is 3.4 eV. The electron temperature was not measured for these experiments, but vacuum ultraviolet spectroscopy of similar SSX plasmas has recently been used to determine $T_e\approx 15$ eV by analysis of the line intensity ratio of carbon III to carbon IV resonant transitions.[19] All of these measurements are made with time resolution and acquisition rate that is faster than the MHD timescale of the plasma.

Figures 1 and 2 show the magnetic structure observed at two times in the evolution of the plasma for a cohelicity merging experiment. The data (vectors) in Fig. 1 show the initial state of the plasma to be mostly axisymmetric and resembling two spheromaks placed next to one another. The toroidal field of each spheromak as well as the reversing poloidal field is evident in the $z=\pm 21.6$ cm data of Fig. 1. This configuration evolves initially via a tilting instability followed by more complex dynamics until it settles into the structure shown in Fig. 2. This structure is clearly not axisymmetric. Instead, the magnetic structure looks like a spheromak inserted at a right angle to the geometric axis of the cylinder:[20] the top left panel (rz plane containing $\theta=45°$) in Fig. 2 resembles the poloidal structure of a spheromak (i.e., the geometric axis of the plasma has aligned with a pair of the magnetic probes), while the top right panel (rz plane containing $\theta=135°$) resembles "toroidal" fields. This picture is, however, not correct; Sec. III will present a more complete model for the structure of this state. Once formed, this structure persists for the lifetime of the plasma.

Fourier analysis of the azimuthal structure shows that this state is dominantly an $m=1$ mode. For example, in the top left rz panel of Fig. 2, B_z changes sign when moving along a diameter across the plasma (i.e., there is a $\cos\theta$ dependence). This is demonstrated in greater detail in Sec.

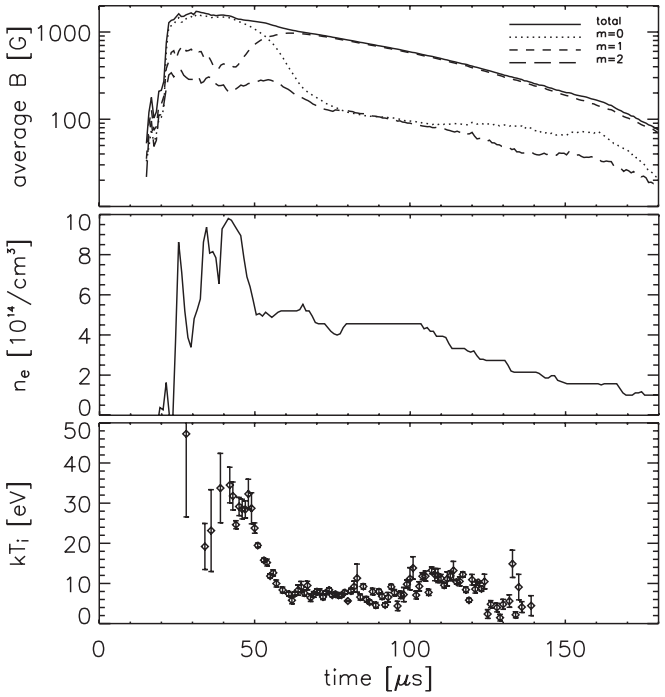

FIG. 3. Time dependence of average B, electron density n_e, and carbon (impurity) ion temperature T_i. Once the relaxed state forms ($t \gtrsim 70$ μs) the plasma has $m=1$ symmetry and self-similarly decays with about a 45 μs e-folding time in B and n_e.

IV. Figure 3(a) collapses the detailed magnetic structure down to the strength in each of the Fourier modes averaged over all the magnetic measurements. The time dependence shown in this figure reveals the dynamical evolution of the plasma from a mostly $m=0$ structure (axisymmetric) to the pure $m=1$ state of Fig. 2, as described above. The time dependences in Fig. 3 of the magnetics, as well as the electron density and ion temperature measurements show that the strong MHD activity present early in the evolution settles once the nonaxisymmetric state forms and the plasma subsequently decays self-similarly without significant fluctuations. The gross characteristics of this relaxed state are $B \approx 1$ kG, $n \approx 4 \times 10^{14}/\mathrm{cm}^3$, and $T_{e,i} \approx 10$ eV, making it a low $\beta < 0.1$ plasma well described by MHD.

Experiments with only one of the plasma guns discharged produce the same final state structure as the cohelicity merging experiments. The initial state shown in Fig. 4(a) is again a mostly axisymmetric state resembling a single spheromak that has not quite filled the entire cylindrical volume. The spheromak begins to tilt and eventually settles to the structure shown in Fig. 4(b), which contains the same features as described for Fig. 2 for the merging experiment.

III. TAYLOR STATES IN A CYLINDRICAL BOUNDARY

Application of Taylor's theory to compact toroidal plasmas produces a direct relationship between the magnetic energy W and total helicity K given by $W=\lambda K/2\mu_0$ (Ref. 9). This means that, of the many possible solutions to $\nabla \times \vec{B} = \lambda \vec{B}$, the Taylor state (minimum magnetic energy) must be the one with the smallest value of λ.

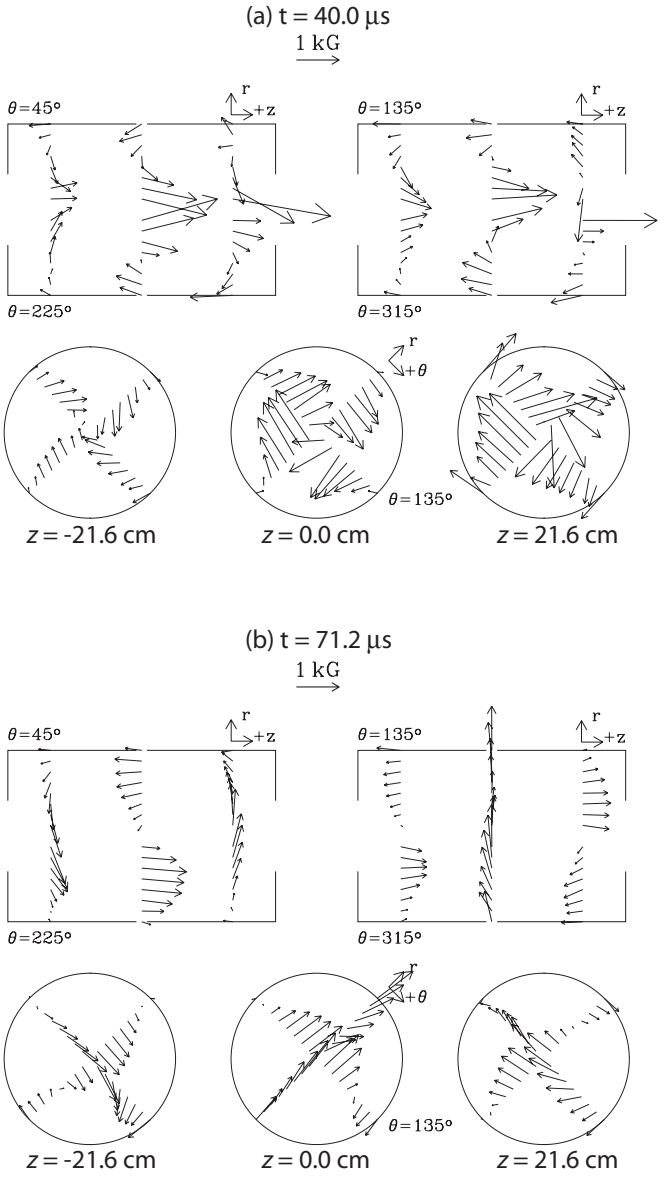

FIG. 4. Measured magnetic structure for single plasma gun discharge. The initial spheromak state (a) is mostly axisymmetric, but the final state (b) is the same (except for an arbitrary global azimuthal rotation) as the nonaxisymmetric relaxed state seen in Fig. 2 for cohelicity merging.

The work in Refs. 13 and 14 made use of these criteria to evaluate the tilt stability of spheromaks, but in doing so this work also effectively determined the Taylor state for any aspect ratio conducting cylinder with no flux at the boundary; this analysis is repeated below. To proceed with the general solution for the Taylor state for arbitrary L/R, the following representation for the magnetic field is assumed:

$$\vec{B} = \hat{z} \times \nabla\psi + \nabla \times (\hat{z} \times \nabla\psi)/\lambda. \tag{2}$$

This transforms $\nabla \times \vec{B} = \lambda \vec{B}$ into a Helmholtz equation $\nabla^2\psi + \lambda^2\psi = 0$, which can be solved by the usual method of separation of variables. The general solution has the form:

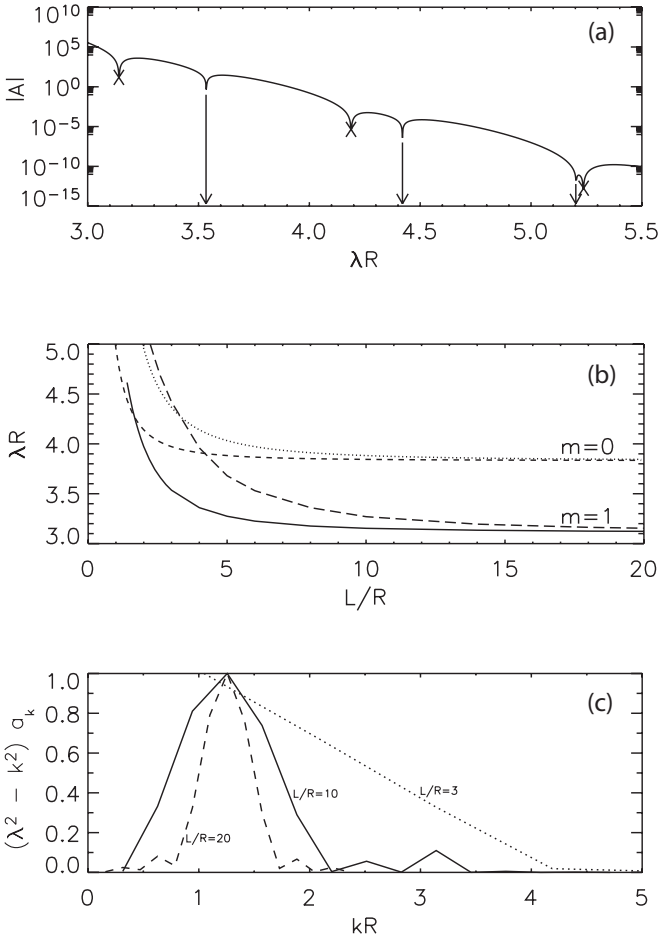

FIG. 5. (a) The determinant of Eq. (4) evaluated for $L/R=3$ and $m=1$. (b) L/R dependence of the values of λR for $m=0$ and $m=1$ solutions. The minimum energy state (smallest λ) is axisymmetric ($m=0$) for $L/R \lesssim 1.67$ and nonaxisymmetric ($m=1$) for $L/R \gtrsim 1.67$). (c) The normalized axial wavenumber (kR) spectrum for the coefficients in the numerical solution [Eq. (3)] for B_z show a narrowing peak around the value $kR \approx 1.23$ with increasing L/R, indicating that the helical structure approaches that of the Taylor double helix solution. The peak value of each spectrum is normalized to one.

$$\psi = \left(\sum_{n=1}^{\infty} a_n J_m(k'r) \sin kz + a_0 r^m e^{i\lambda z} \right) e^{im\theta}, \tag{3}$$

where $k=n\pi/L$ and $k'=(\lambda^2-k^2)^{1/2}$, and the ends of the cylinder are taken to be at $z=0,L$. Application of the boundary condition $B_r(R)=0$ produces the following condition for any z:

$$\sum_{n=1}^{\infty} a_n \left[\frac{im}{R} J_m(k'R) \sin kz + \frac{kk'}{\lambda} J'_m(k'R) \cos kz \right] + 2ima_0 R^{m-1} e^{ikz} = 0. \tag{4}$$

Truncating the summation at finite order N and evaluating at $2N+1$ locations in z produces a linear system of equations that is evidently a null mapping of the coefficients a_n. The condition that the determinant must be zero therefore specifies possible values of λ. Figure 5(a) shows the determinant evaluated as a function of λ for $L/R=3$ and $m=1$. Two valid solutions at $\lambda R=3.53$ and $\lambda R=4.40$ are shown (there are however an infinite number of solutions); there are also spurious roots appearing at $\lambda=n\pi/L$. Once a valid λ is determined, the corresponding a_n needed to compute the fields can be evaluated by using the same system of equations.

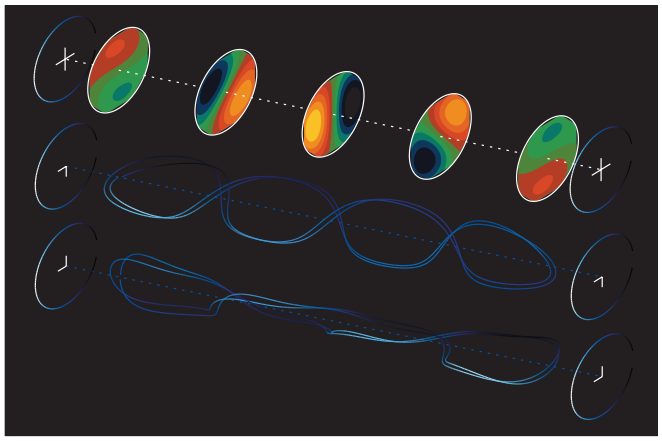

FIG. 6. (Color) B_z isosurfaces for the $L/R=10$ Taylor state (top) and two orthogonal views (middle and bottom) of a field line to illustrate the helical character of the structure and the simplified description of the structure as a twisted closed loop of flux. The dotted line is the cylindrical axis; the perpendicular line segments on the end walls (circles) indicate the $\pi/2$ rotation between the two views of the field lines.

Figure 5(b) shows the result of the above analysis for $L/R<20$. The two smallest values of λ for solutions with $m=0$ and $m=1$ symmetry are shown; none of the other symmetries $m \geq 2$ have smaller values of λ. The minimum energy Taylor state is therefore seen to be axisymmetric only for values of $L/R \lesssim 1.67$. For $L/R \gtrsim 1.67$ the minimum energy state is predicted to have a pure $m=1$ symmetry.

The structure of Taylor states with $L/R=10$ and $L/R=3$ is shown in Figs. 6 and 7. Evidently, the essential aspect of the structure of these states is their helical character. The $m=1$ symmetry is simply a necessary ingredient of the helical structure. These states can be pictured as a closed loop of flux that has been flattened (opposite sides of the loop brought together so that it may be fit into the cylindrical boundary), and then twisted. In this picture, the positively and negatively signed isosurfaces of B_z shown in either Fig. 6 or Fig. 7 correspond to the flux from opposing sides of the loop that have been pushed against one another and the helical rotation of these structures corresponds to the twist of the loop.

The pitch of the twist is, however, not arbitrary. As L/R gets larger, the structure approaches that of a pure helical wavenumber $kR \approx 1.23$. Figure 5(c) shows the k dependence of the coefficients a_n in the expansion of B_z obtained from the numerical analysis described above. The spectrum clearly narrows with increasing L/R, and the breadth of the spectrum for finite L/R simply reflects the relative importance of the finite length of the plasma. The solution for infinite L/R becomes the same as the cylindrical approximation of the RFP with zero axial (toroidal) flux, which is known to be the Taylor "double helix" solution that has a pure $\cos(kz+\theta)$ dependence with $kR \approx 1.23$.[9,21] Note that the value of λR in Fig. 5(b) approaches 3.11 at large L/R, which corresponds to

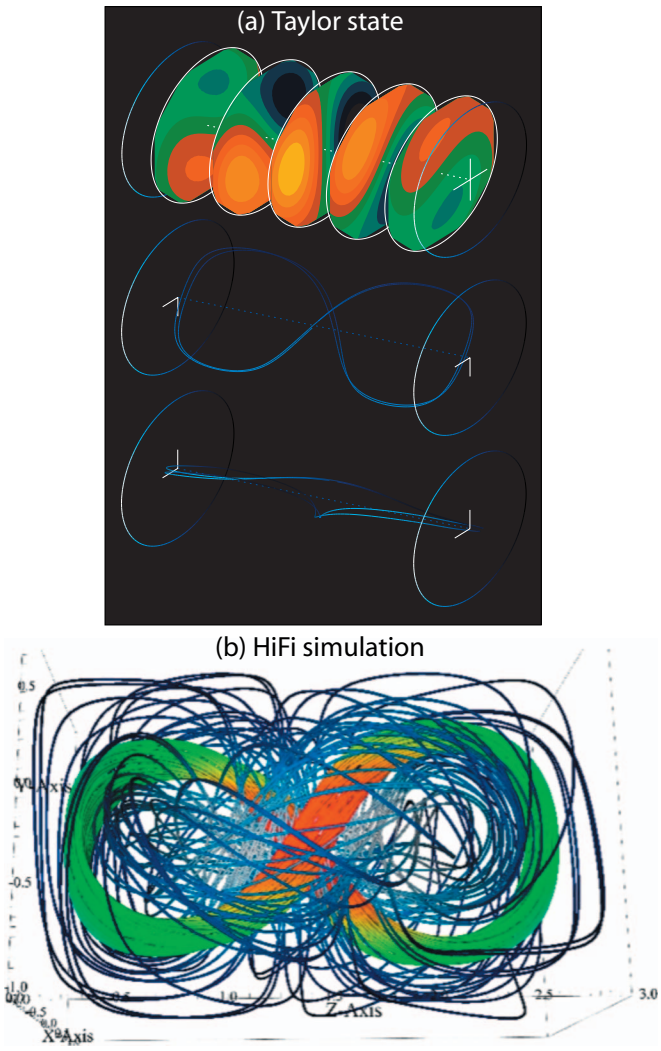

FIG. 7. (Color) (a) B_z isosurfaces for the $L/R=3$ Taylor state and two orthogonal views of a field line to illustrate the helical character of the structure. (b) Field lines drawn through the final state of an MHD simulation using the HiFi (Refs. 23) code initialized with the Bessel function double-spheromak state. The final state is consistent with the Taylor state structure. The cylindrical boundary is not shown in (b) but is in roughly the same horizontal orientation as the figures in (a).

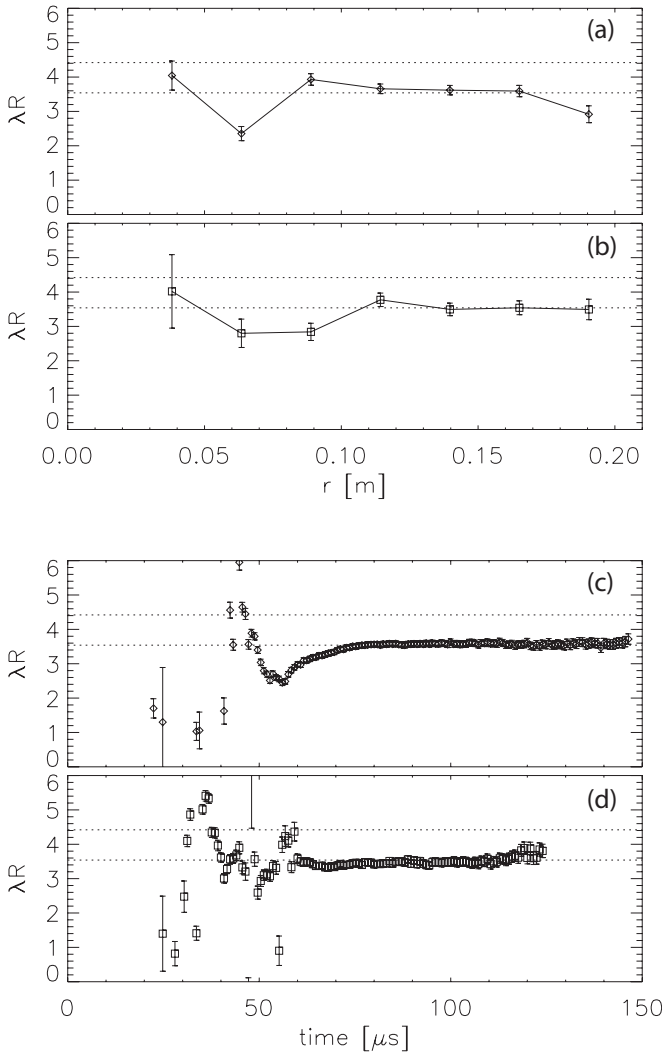

FIG. 8. Measurements of λ for the cohelicity merging experiment [(a) and (c)] and for the single plasma gun discharge (single spheromak) experiment [(b) and (d)]. The radial profiles of λR [(a) and (b)] are consistent with the Taylor state value (lower dotted line at $\lambda R=3.53$); the next larger value $\lambda R=4.40$ giving an $m=1$ state (see Fig. 5) is indicated by the upper dotted line. The radial average of λ (excluding the two values at smallest r) stays very near the Taylor state value throughout the decay of the nonaxisymmetric self-organized state [(c) and (d)]. Figure adapted from Ref. 12.

the value at which the RFP Taylor states also have a transition to nonaxisymmetric solutions.

The numerical solutions described above were found to be in very good agreement with a computation using the PSI-TET code.[22] In addition, the HiFi code[23] was used to follow the dynamical evolution of the cohelicity merging process using the second order Bessel function (double) spheromak solution as the initial state. The final state shown in Fig. 7(b) is seen to be in good agreement with the Taylor state. Details of the dynamics of this process are described in Ref. 24.

IV. RESULTS

The experimental measurements can now be compared in detail to the predictions of the Taylor theory. In particular, if the plasma is magnetically relaxed, it should have a flat spatial profile of λ with a value predicted to be $\lambda R=3.53$ from the above analysis, which for the $R=0.2$ m cylinder used in the experiment gives $\lambda=17.7\ \mathrm{m}^{-1}$. Note that λ may be expressed as

$$\lambda=\frac{1}{B_z}\left[\frac{1}{r}\frac{\partial}{\partial r}(rB_\theta)+\frac{1}{r}\frac{\partial B_r}{\partial\theta}\right]. \tag{5}$$

The data permit a determination of λ if the $m>1$ contributions are neglected so that the azimuthal Fourier analysis using only the resolved $m=0$ and $m=1$ modes are used to compute θ derivatives. Figures 8(a) and 8(b) show the results of such an analysis for both cohelicity merging and for a single spheromak initial state. The λ profile is indeed relatively flat for both initial experimental conditions, and consistent with the minimum energy Taylor state value $\lambda R=3.53$ ($\lambda=17.7\ \mathrm{m}^{-1}$). For comparison, the value $\lambda R=4.40$

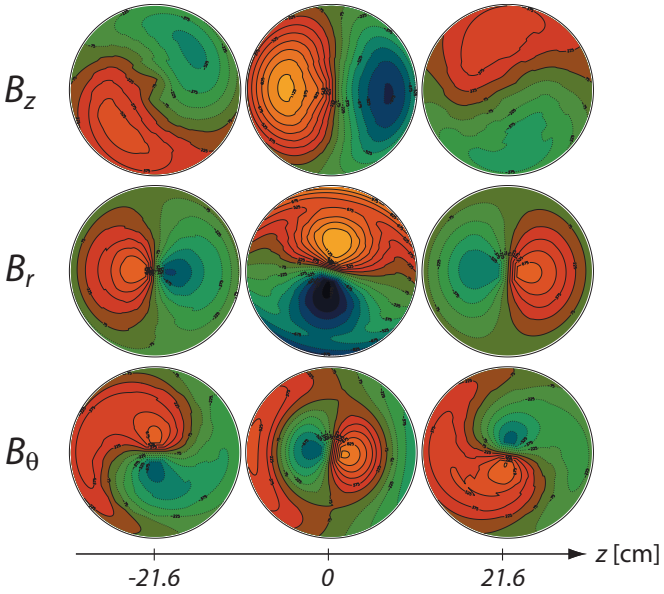

FIG. 9. (Color) Contour plots of B_z, B_r, and B_θ determined experimentally (corresponding to the data of Fig. 2). Isosurfaces are separated by 150 G. Red/yellow colors (solid lines) are positive values; blue/green (dotted lines) are negative values. Figure adapted from Ref. 12.

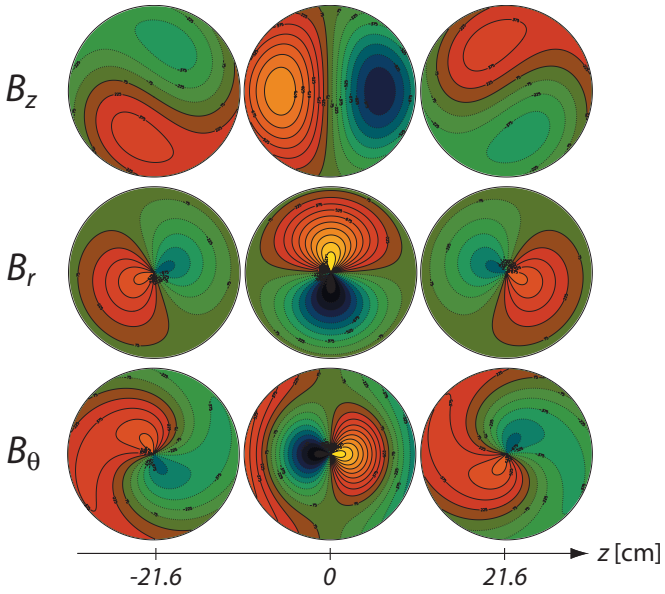

FIG. 10. (Color) Contour plots of B_z, B_r, and B_θ for the calculated Taylor state with $L/R=3$. The only free parameter is the total helicity, which was adjusted to give best agreement with the experimental results. Isosurfaces are separated by 150 G. Red/yellow colors (solid lines) are positive values; blue/green (dotted lines) are negative values. Figure adapted from Ref. 12.

from Fig. 5(a) for the next higher $m=1$ solution is clearly incompatible with the experimental data (upper dashed lines in each part of this figure). Figures 8(c) and 8(d) show that the value of λ remains steady once the relaxed state is formed, also for both initial conditions. In this context, it is worth noting the large amount of resistive decay evident in Fig. 3.

To better understand the measured structure and compare to the Taylor state calculations, the azimuthal Fourier decomposition (dropping the $m=2$ mode) is once again used to generate the contour plots of B_z, B_r, and B_θ displayed in Fig. 9. The dominance of the $m=1$ mode is now clearly evident in the positive (red/yellow) and negative (blue/green) structures in each r-θ plane, consistent with the prediction of a pure $m=1$ symmetry for the Taylor state. Furthermore, moving along the cylindrical axis, the lobes of closed contours seen in all components clearly rotate in θ, indicating that the structure is helical. There is about a half-twist (π rotation) resolved in the data. The oppositely signed lobes are consistent with the picture developed for the general structure for Taylor states with large L/R; for example, a flux tube associated with the positive lobes of B_z followed from one end of the cylinder will turn around at the other end and become the adjacent negative lobes.

Figure 10 shows the Taylor state structure for $L/R=3$ displayed in the same manner as the experimental data in Fig. 9. The agreement is evidently quite good. The total helicity is the only free parameter, which was adjusted to give the best visual agreement with the data (in principle there is an additional global azimuthal rotation required, but the plasma tended to align itself with a pair of the magnetic probes so the orientation of the Taylor state was straightforward).

V. DISCUSSION AND SUMMARY

Because the same helically distorted, nonaxisymmetric stable CT plasma emerges in the final state for two very different initial states, i.e., not only for the two-spheromak cohelicity merging experiments but also for the one-spheromak single plasma gun discharge experiments, it seems likely that some self-organization process is at work. Both plasmas evolve to structure characterized by the longest length scale of the system, a behavior typical of self-organization. For cohelicity merging, the two spheromaks in the initial state have a characteristic length no larger than half the length of the cylinder and clearly evolve to a state that relaxes into the full length of the cylinder. The two initial states possible with this experiment are approximately the two lowest order Bessel function model spheromak states, which have values $\lambda R=3.98$ and 4.36, respectively. Since $1/\lambda$ is a length scale, the helically distorted nonaxisymmetric relaxed state with $\lambda R=3.53$ clearly has a larger characteristic scale length than either initial states. The behavior of these plasmas in three-dimensional MHD is somewhat analogous to the inverse cascade which gives rise to large scale structure in two-dimensional fluid turbulence. While there is no evidence for the turbulent relaxation process Taylor envisioned in order reach the relaxed state quickly, the excellent agreement of the experimental data with the computed Taylor state likely means that the self-organizing processes do conserve the total magnetic helicity.

The lifetime of this CT is comparable to or greater than the lifetime of other CTs produced at SSX. The FRC-like object resulting from counterhelicity merging[17] always was tilt unstable, but the axisymmetric "dipole-trapped" spheromak[25] state decayed with an e-folding time for B of about 30 μs, less than the 45 μs timescale for the decay of

the nonaxisymmetric CT. This comparison suggests the nonaxisymmetry of the configuration does not negatively impact its confinement properties. However, the resistive decay timescale may be computed using the Taylor state properties to be $\tau^{-1}=\lambda^2\eta/2\mu_0$, which gives the significantly longer timescale $\tau=510$ μs for $T_e=10$ eV ($\tau=180$ μs for $T_e=5$ eV).

To summarize, this paper describes the magnetic self-organization of a nonaxisymmetric CT plasma. For both one- and two-spheromak initial conditions, the plasma spontaneously evolves to the same helically distorted stable MHD equilibrium with $m=1$ azimuthal symmetry. The flat spatial profile of λ measured for this CT shows that it is a magnetically relaxed plasma. Because the internal magnetic structure agrees well with the predicted Taylor relaxed state, the total helicity is likely a robust invariant. The structure of this CT can be described as the Taylor double helix with finite length effects or as a tilted and twisted spheromak.

ACKNOWLEDGMENTS

This research was supported by the U.S. Department of Energy grant No. DE-FG02-00ER54604 and Plasma Science and Innovation Center (PSI-Center), the National Science Foundation Physics Frontier Center for Magnetic Self Organization (CMSO), and the Office of Naval Research.

[1]M. N. Rosenbluth and M. N. Bussac, Nucl. Fusion **19**, 489 (1979).
[2]T. R. Jarboe, I. Henins, H. W. Hoida, R. K. Linford, J. Marshall, D. A. Platts, and A. R. Sherwood, Phys. Rev. Lett. **45**, 1264 (1980).
[3]G. C. Goldenbaum, J. H. Irby, Y. P. Chong, and G. W. Hart, Phys. Rev. Lett. **44**, 393 (1980).
[4]T. R. Jarboe, Plasma Phys. Controlled Fusion **36**, 945 (1994).
[5]P. M. Bellan, *Spheromaks* (Imperial College Press, London, 2000).
[6]H. A. B. Bodin and A. A. Newton, Nucl. Fusion **20**, 1255 (1980).
[7]R. J. La Haye, T. H. Jensen, P. S. C. Lee, R. W. Moore, and T. Ohkawa, Nucl. Fusion **26**, 255 (1986).
[8]J. B. Taylor, Phys. Rev. Lett. **33**, 1139 (1974).
[9]J. B. Taylor, Rev. Mod. Phys. **58**, 741 (1986).
[10]A. Hasegawa, Adv. Phys. **34**, 1 (1985).
[11]D. Montgomery, W. H. Matthaeus, W. T. Stribling, D. Martinez, and S. Oughton, Phys. Fluids A **4**, 3 (1992).
[12]C. D. Cothran, M. R. Brown, T. Gray, M. J. Schaffer, and G. Marklin, Phys. Rev. Lett. **103**, 215002 (2009).
[13]J. M. Finn, W. Manheimer, and E. Ott, Phys. Fluids **24**, 1336 (1981).
[14]A. Bondeson, G. Marklin, Z. G. An, H. H. Chen, Y. C. Lee, and C. S. Liu, Phys. Fluids **24**, 1682 (1981).
[15]M. R. Brown, Phys. Plasmas **6**, 1717 (1999).
[16]A. Reiman, Phys. Fluids **25**, 1885 (1982).
[17]C. D. Cothran, A. Falk, A. Fefferman, M. Landreman, M. R. Brown, and M. J. Schafffer, Phys. Plasmas **10**, 1748 (2003).
[18]C. D. Cothran, J. Fung, M. R. Brown, and M. J. Schaffer, Rev. Sci. Instrum. **77**, 063504 (2006).
[19]V. Chaplin, M. R. Brown, D. H. Cohen, T. Gray, and C. D. Cothran, Phys. Plasmas **16**, 042505 (2009).
[20]T. R. Jarboe, I. Henins, A. R. Sherwood, C. W. Barnes, and H. W. Hoida, Phys. Rev. Lett. **51**, 39 (1983).
[21]M. J. Schaffer, Phys. Fluids **30**, 160 (1987).
[22]T. R. Jarboe, W. T. Hamp, G. J. Marklin, B. A. Nelson, R. G. O'Neill, A. J. Redd, P. E. Sieck, R. J. Smith, and J. S. Wrobel, Phys. Rev. Lett. **97**, 115003 (2006).
[23]V. S. Lukin, Ph.D. thesis, Princeton University, 2007.
[24]T. Gray, M. R. Brown, C. D. Cothran, V. S. Lukin, G. Marklin, and M. J. Schaffer, "Evolution to a minimum energy Taylor state in multiple flux conserving boundaries in SSX," Phys. Plasmas (submitted).
[25]M. R. Brown, C. D. Cothran, J. Fung, M. Chang, J. Horwitz, M. J. Schaffer, J. Leuer, and E. V. Belova, Phys. Plasmas **13**, 102503 (2006).